

ORIGINAL ARTICLE

OPEN

Loss of hepatic SMLR1 causes hepatosteatosis and protects against atherosclerosis due to decreased hepatic VLDL secretion

Willemien van Zwol¹  | Antoine Rimbart²  | Justina C. Wolters¹ |
 Marieke Smit¹ | Vincent W. Bloks¹ | Niels J. Kloosterhuis¹ |
 Nicolette C. A. Huijkman¹ | Mirjam H. Koster¹ | Umesh Tharehalli¹ |
 Simon M. de Neck³ | Colin Bournez⁴ | Marceline M. Fuh⁵ | Jeroen Kuipers⁶ |
 Sujith Rajan⁷ | Alain de Bruin^{1,3} | Henry N. Ginsberg⁸ |
 Gerard J. P. van Westen⁴  | M. Mahmood Hussain⁷ | Ludger Scheja⁵ |
 Joerg Heeren⁵ | Philip Zimmerman⁹ | Bart van de Sluis¹ | Jan Albert Kuivenhoven¹

¹Department of Pediatrics, University Medical Center Groningen, University of Groningen, Groningen, the Netherlands

²Université de Nantes, CNRS, INSERM, l'institut du thorax, Nantes, France

³Department of Biomolecular Health Sciences, Faculty of Veterinary Medicine, Utrecht University, Utrecht, the Netherlands

⁴Division of Drug Discovery and Safety, Leiden Academic Center for Drug Research, Leiden University, Leiden, The Netherlands

⁵Department of Biochemistry and Molecular Cell Biology, University Medical Center Hamburg-Eppendorf, Hamburg, Germany

⁶Department of Biomedical Sciences of Cells and Systems, University of Groningen, University Medical Center Groningen, Groningen, the Netherlands

⁷Department of Foundations of Medicine, NYU Long Island School of Medicine, Mineola, New York, USA

⁸Department of Medicine, Columbia University, Vagelos College of Physicians and Surgeons, New York, New York, USA

⁹NEBION AG, Zurich, Switzerland

Correspondence

Jan Albert Kuivenhoven, Department of Laboratory Medicine, University Medical Center Groningen, University of Groningen, 9713 AV Groningen, the Netherlands.
 Email: j.a.kuivenhoven@umcg.nl

Funding information

Deutsche Forschungsgemeinschaft, Grant/Award Number: SFB 841 and B6; European Union, acronym EndoConnect, Grant/Award Number: MSCA-ITN- 2020 and 953489; Hartstichting, Grant/ Award Number: 2015T068; National Institutes of Health, Grant/Award Number: 5R35HL135833, DK121490,

Abstract

Background and Aims: The assembly and secretion of VLDL from the liver, a pathway that affects hepatic and plasma lipids, remains incompletely understood. We set out to identify players in the VLDL biogenesis pathway by identifying genes that are co-expressed with the *MTTP* gene that encodes for microsomal triglyceride transfer protein, key to the lipidation of apolipoprotein B, the core protein of VLDL. Using human and murine transcriptomic data sets, we identified small leucine-rich protein 1 (*SMLR1*), encoding for small leucine-rich protein 1, a protein of unknown function that is exclusively expressed in liver and small intestine.

Abbreviations: AAV, adeno-associated virus; APOB, apolipoprotein B; AV, adenovirus; Cas9, CRISPR-associated protein 9; ER, endoplasmic reticulum; GoF, gain-of-function; H&E, hematoxylin and eosin; HFD, High-fat, high-cholesterol diet; hSMLR1, human SMLR1; IHH, immortalized human hepatocyte; IR, insulin receptor; MTP, microsomal triglyceride transfer protein; NAS, NAFLD activity score; sgRNA, single-guide RNA; Smlr1, small leucine-rich protein 1; Smlr1-LKO, liver-specific knockout of Smlr1; TAG, triacylglycerol; TC, total cholesterol; TG, triglyceride; VTV, VLDL transport vesicle.

Philip Zimmerman, Bart van de Sluis, and Jan Albert Kuivenhoven contributed equally to this work. www.hepjournal.com.

Supplemental Digital Content is available for this article. Direct URL citations appear in the printed text and are provided in the HTML and PDF versions of this article on the journal's website, www.hepjournal.com.

This is an open access article distributed under the terms of the Creative Commons Attribution-Non Commercial-No Derivatives License 4.0 (CCBY-NC-ND), where it is permissible to download and share the work provided it is properly cited. The work cannot be changed in any way or used commercially without permission from the journal.

Copyright © 2023 The Author(s). Published by Wolters Kluwer Health, Inc.

HL137202, HL158054 and R01 DK118480; Netherlands CardioVascular Research Initiative, acronym GeniusII, Grant/ Award Number: CVON2017-2020; State of Hamburg, Grant/Award Number: LFF-FV75; Stichting De Cock-Hadders, Grant/ Award Number: 2020-69

Approach and Results: To assess the role of SMLR1 in the liver, we used somatic CRISPR/CRISPR-associated protein 9 gene editing to silence murine *Smlr1* in hepatocytes (*Smlr1*-LKO). When fed a chow diet, male and female mice show hepatic steatosis, reduced plasma apolipoprotein B and triglycerides, and reduced VLDL secretion without affecting microsomal triglyceride transfer protein activity. Immunofluorescence studies show that SMLR1 is in the endoplasmic reticulum and Cis-Golgi complex. The loss of hepatic SMLR1 in female mice protects against diet-induced hyperlipidemia and atherosclerosis but causes NASH. On a high-fat, high-cholesterol diet, insulin and glucose tolerance tests did not reveal differences in male *Smlr1*-LKO mice versus controls.

Conclusions: We propose a role for SMLR1 in the trafficking of VLDL from the endoplasmic reticulum to the Cis-Golgi complex. While this study uncovers SMLR1 as a player in the VLDL assembly, trafficking, and secretion pathway, it also shows that NASH can occur with undisturbed glucose homeostasis and atheroprotection.

INTRODUCTION

The assembly and secretion of VLDL, consisting of apolipoprotein B (apoB) with cholesterol, triglycerides (TGs), and phospholipids, plays a pivotal role in hepatic lipid homeostasis. The latter is clearly illustrated by the development of NAFLD in patients with truncating mutations in apoB, or patients who lack the microsomal triglyceride transfer protein (MTP), which is required for the lipidation of apoB.^[1] Reduced VLDL secretion is, on the other hand, associated with reduced plasma lipids and atherosclerosis.^[2] Increasing insight into VLDL biogenesis is therefore relevant to obese patients who often present NAFLD as well as atherosclerotic cardiovascular disease.

Studies into the biogenesis of VLDL have generally centered on apoB. Although there is evidence that apoB levels are regulated at the mRNA level,^[3,4] most studies support regulation at the posttranscriptional level.^[5] Following stabilization of apoB in the endoplasmic reticulum (ER),^[6] MTP initiates the transfer of phospholipids and TGs to apoB (for a detailed description, see Sirwi et al.^[7]). Over the last few years, however, it has become clear that lipidation of apoB is a complex process that is not solely dependent on MTP activity but on a range of ER-resident proteins including prolinerich acidic protein 1, torsinA, transmembrane 6 superfamily member 2 (TM6SF2), transmembrane 41B (TMEM41B), and vacuole membrane protein 1.^[8-13] Most of this insight comes from experimental mouse studies but there is evidence that the expression of several of the respective genes is altered in patients with NAFLD versus controls.^[8,9] Carriers of functional mutations in *TM6SF2* are, for example, characterized by reduced VLDL secretion and increased risk for NAFLD.^[14]

After the formation of VLDL at the ER, the nascent particle is transported to the Golgi through the so-called

VLDL transport vesicle (VTV).^[15] In addition to the coatamer complex II proteins, required for all intracellular protein transport, it has been shown that several proteins specifically mediate this VTV transport, which includes small VCP interacting protein, cell deathinducing DFF4-5like effector b, reticulon 3, and transport and Golgi organization 1, with surfeit 4 (SURF4) as latest member on this block.^[15-18] For the subsequent docking of VTVs at the cis-Golgi, a role for the SNARE proteins has been suggested.^[19] How VLDL is transported further from the Cis-Golgi to the Trans-Golgi, and from there to the cell membrane for subsequent secretion, remains elusive.

Using co-expression analyses, we identified small leucine-rich protein 1 (*SMLR1*), encoding small leucine-rich protein 1, a protein of unknown function, to be contextually co-expressed with *MTP*. Here we show that hepatic loss of *Smlr1* in mice reduces VLDL secretion and prevents diet-induced atherosclerosis but causes hepatosteatosis (NAFLD and NASH) without affecting glucose homeostasis.

METHODS

Animal model

All studies were approved by the Institutional Animal Care and Use Committee, University of Groningen (Groningen, the Netherlands) and are in line with the Guide for the Care and Use of Laboratory Animals. We generated *Smlr1* knockout mice (*Smlr1*^{-/-}) using CRISPR/CRISPR-associated protein 9 (Cas9) technology, as described previously.^[20]

C57BL/6J male and female mice with hepatocyte-specific Cas9 expression, received retro-orbital

administration of either 0.5×10^{11} adenovirus or 1×10^{11} adeno-associated virus 8 (AAV8),^[21] harboring three single-guide RNAs (sgRNAs) (Figure S3) targeting *Smlr1* or a matched viral dose containing scaffold sgRNA. At the start of the experiments, mice were 10–12 weeks of age, single housed in ventilated cages with cage enrichment in a climate-controlled room with a 12-h light/12-h dark cycle lighting regime and fed *ad libitum* with chow diet (RM1, Special Diet Services). Female mice were sensitized for atherosclerosis development via additional injection with 3×10^{11} AAV8 particles containing a PCSK9 gain-of-function variant and fed a high-fat, high-cholesterol diet (HFD, 60%, 0.25%, respectively; D14010701; Research Diet).^[22] Male mice used for the glucose and insulin tolerance test also received HFD.

Animal experiments

Interventions were performed during the light cycle. Blood was collected after a 5-h morning fasting period by retro-orbital bleeding or after sacrifice using cardiac puncture under anesthesia. Plasma was spun down at 1000 g for 10 min at 4°C and stored at –80°C until further analysis. After sacrifice, a liver part and the whole heart were harvested, washed in PBS, and fixed in 4 % (wt/vol) paraformaldehyde, embedded in paraffin, and sectioned at 4 μm. The other liver parts were snap-frozen in liquid nitrogen and stored at –80°C until further analysis.

Statistical analysis

Analyses were performed using GraphPad Prism version 9.0.0. Unpaired two-tailed Student's *t* test was used to compare groups. Two-way ANOVA with multiple comparisons was used to assess TG levels or glucose levels at different time points. Data represent mean ± SEM unless otherwise specified. For all experiments, a *p* value < 0.05 was considered statistically significant. Asterisks denote corresponding statistical significance: **p* < 0.05, ***p* < 0.005, and ****p* < 0.0005.

Other procedures are described in the [Supporting Information](#).

RESULTS

Identification of a lipid candidate gene via contextual co-expression analyses

In different fields of research, it has been shown that genes encoding for proteins involved in common pathways tend to show similar mRNA expression patterns.^[23,24] In this light, we used contextual co-expression analysis as a tool to find uncharacterized

genes that might play roles in VLDL assembly and secretion, starting with *MTTP* as the central gene. Using the large-scale expression data from RNA-sequencing (RNA-seq) platforms and microarray compendium data in GENEVESTIGATOR, we selected the top 25 genes most highly co-expressed with *MTTP* across all samples from the selected compendium. Additionally, co-expression was also run across tissues (anatomy) and conditions (perturbations), where each tissue or condition represents an aggregated value obtained from the corresponding samples. Seven genes besides *MTTP* were found overlapping, including *SMLR1*, solute carrier family 2 member 2, *APOB*, *apolipoprotein C3 (APOC3)*, *apolipoprotein A1 (APOA1)*, *phospholipase A2 group XIIB (PLA2G12B)*, and *RNA U1 small nuclear 70 (Figure 1A)*. Among these, the apolipoproteins are well-established players in lipid metabolism,^[25] while *PLA2G12B* was recently shown to be involved in VLDL and triglyceride metabolism.^[26] In other words, the unknown genes in our list may very well also have a role in lipid metabolism. There was no information in the public domain following identification of *SMLR1*. Because *SMLR1* was also listed using three independent technologies and compendia including Illumina RNA-seq, Agilent arrays and Affymetrix arrays (Figure S1), and murine *Smlr1* also showed co-expressed with *Mttp*, we chose to further characterize *SMLR1* and hypothesize a role for *SMLR1* in the metabolism of apoB-containing lipoproteins.

SMLR1 is almost exclusively expressed in the liver and in small intestine (Figure 1B) and encodes a *SMLR1* of 107 amino acids in humans (UniProtKB; H3BR10). We constructed an atomic-resolution model of human *SMLR1* (h*SMLR1*) (see Methods). In addition to two putative transmembrane helix domains (Figure 1C), it appears that the residue just after the second transmembrane region is in a mobile loop without a specific indication of a ligand or protein binding area. The C-terminal part of the human protein is highly conserved across species (Figure 1D). Mouse *SMLR1* lacks the N-terminal portion of the human isoform and is predicted to encompass one transmembrane helix that bears 85.3% sequence similarity to that of the human C-terminal domain (Figure S2).

Hepatic *Smlr1* deficiency reduces plasma lipids in mice fed a chow diet

To validate *Smlr1* as a lipid gene, we set out to generate whole-body *Smlr1* knockout mice (*Smlr1*^{−/−}) but the absence of homozygous *Smlr1* null mice in the offspring of intercrosses between heterozygous *Smlr1* (*Smlr1*^{+/-}) knockout mice indicated that a complete loss of *Smlr1* is embryonically lethal. However, the heterozygous mice did not present any apparent phenotype (data not shown). In a next step, we deleted *Smlr1* in hepatocytes using somatic CRISPR/Cas9 gene editing (Figure S3). Six weeks after virus administration, mice that received

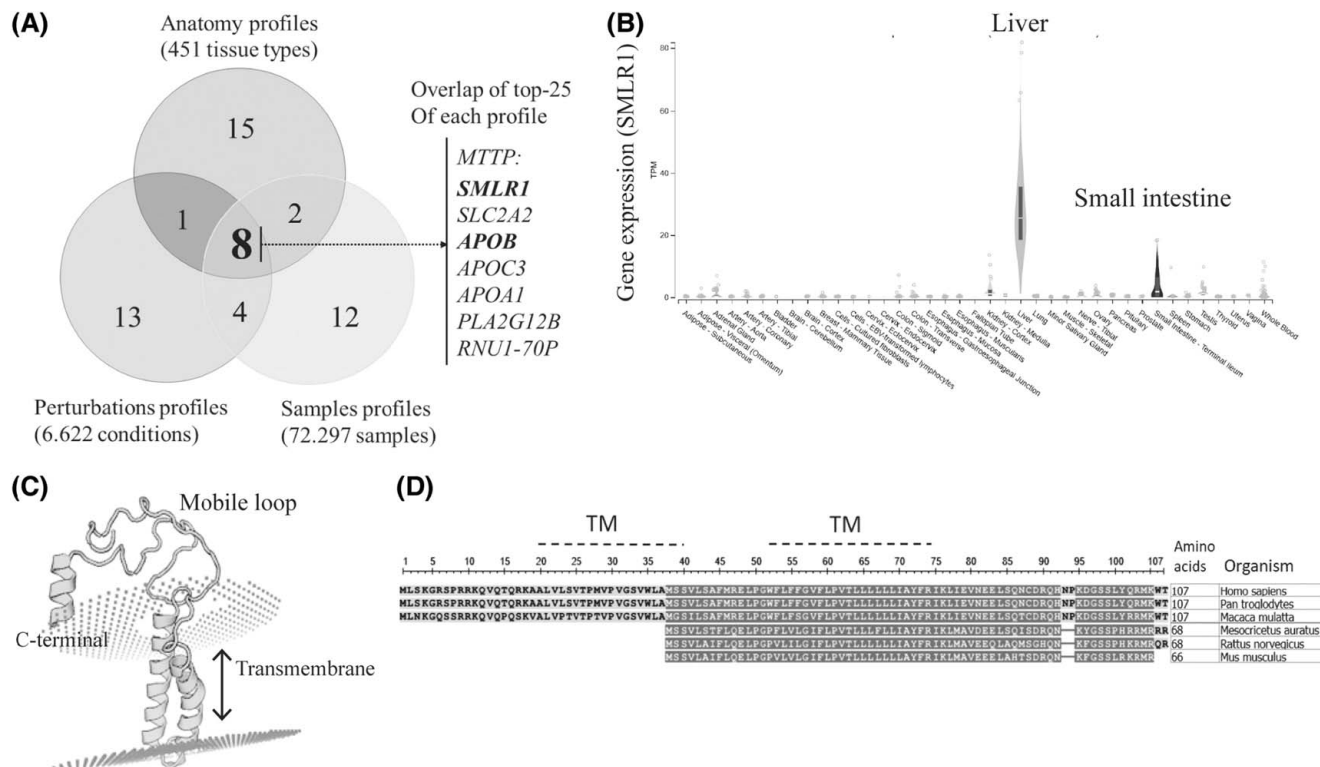


FIGURE 1 Target discovery approach and predicted gene expression and 3D modeling of SMLR1. (A) Top 25 genes co-expressed with *MTTP* by anatomical, perturbational, and sample profiles from curated databases. The profiles represent average expression by tissue type, log ratios of expression by perturbation, and sample-level expression as compiled from a curated compendium of 72,297 Affymetrix Human 133 Plus 2 microarrays. (B) Gene-expression profile from GTExPortal ENSG000002576162.2. (C) Predictive modeling of human small leucine-rich protein 1 (hSMLR1) with use of the protein data bank structure 6RX4 chain B. (D) Interspecies conservation of hSMLR1. Blocks indicate highly conserved regions. Abbreviations: APOA1, apolipoprotein A1; APOB, apolipoprotein B; APOC3, apolipoprotein C3; PLA2G12B, phospholipase A2 group XIIIB; RNU1-170P, RNA U1 small nuclear 70; SLC2A2, solute carrier family 2 member 2; TM, transmembrane

sgRNAs targeting *Smlr1* (liver-specific knockout [*Smlr1*-LKO]) showed a 93% reduction of *Smlr1* mRNA compared with controls (Figure 2A). In the absence of available antibodies, we established a targeted mass-spectrometry assay and showed an 82% down-regulation of SMLR1 protein (Figure 2B). Over the course of the experiment, no significant changes in body weight and food intake were seen in *Smlr1*-LKO mice compared with control mice on chow (Figure S4A, B). However, *Smlr1*-LKO male mice presented a marked reduction of 56% in cholesterol and 52% in triglyceride plasma levels compared with controls (Figure 2C,D). Similar results were obtained in female *Smlr1*-LKO mice (Figure S5A-E), and in subsequent experiments we used male or female mice, dependent on the research question. Fast protein liquid chromatography lipoprotein profiling of pooled plasma samples of *Smlr1*-LKO mice revealed pronounced decreases of cholesterol in LDL and HDL (Figure 2C), and a drop of TG in VLDL (Figure 2D). In addition, a plasma lipidomics survey showed decreases in nearly all (high-abundant and low-abundant) major lipid species in *Smlr1*-LKO mice compared with controls. The most notable differences were seen for cholesterol esters (-32%), phosphatidylcholine (-67%), triacylglycerol (TAG;

-55%), and ceramides (-67%) (Figure 2E). These combined findings validate *Smlr1* as a lipid gene required for plasma lipid homeostasis and show that contextual co-expression analysis is a valuable tool to identify genes through the study of genes with known function, in this case *MTTP*.

Hepatic SMLR1 deficiency induces hepatic steatosis in mice fed a chow diet

On a regular chow diet, the marked reduction of fasting plasma lipids in mice lacking hepatic SMLR1 compared with controls prompted us to study liver lipid homeostasis, as blocking the VLDL secretion pathway often results in hepatic steatosis.^[10,16,27] *Smlr1*-LKO mice showed an increase in liver weight, liver/body weight ratio (Figure 3A, Figure S4C), and a 1.6-fold and 6.8-fold increase in hepatic cholesterol and triglycerides, respectively, compared with controls (Figure 3B,C). Lipidomics validated a marked hepatic accumulation of TAG content (Figure 3D), a hallmark for hepatic steatosis.^[28] Other major lipid species were also increased, with 5.8-fold, 1.6-fold, and 1.4-fold increases in cholesterol esters, diacylglycerols, and phosphatidylethanolamines, respectively (Figure 3D).

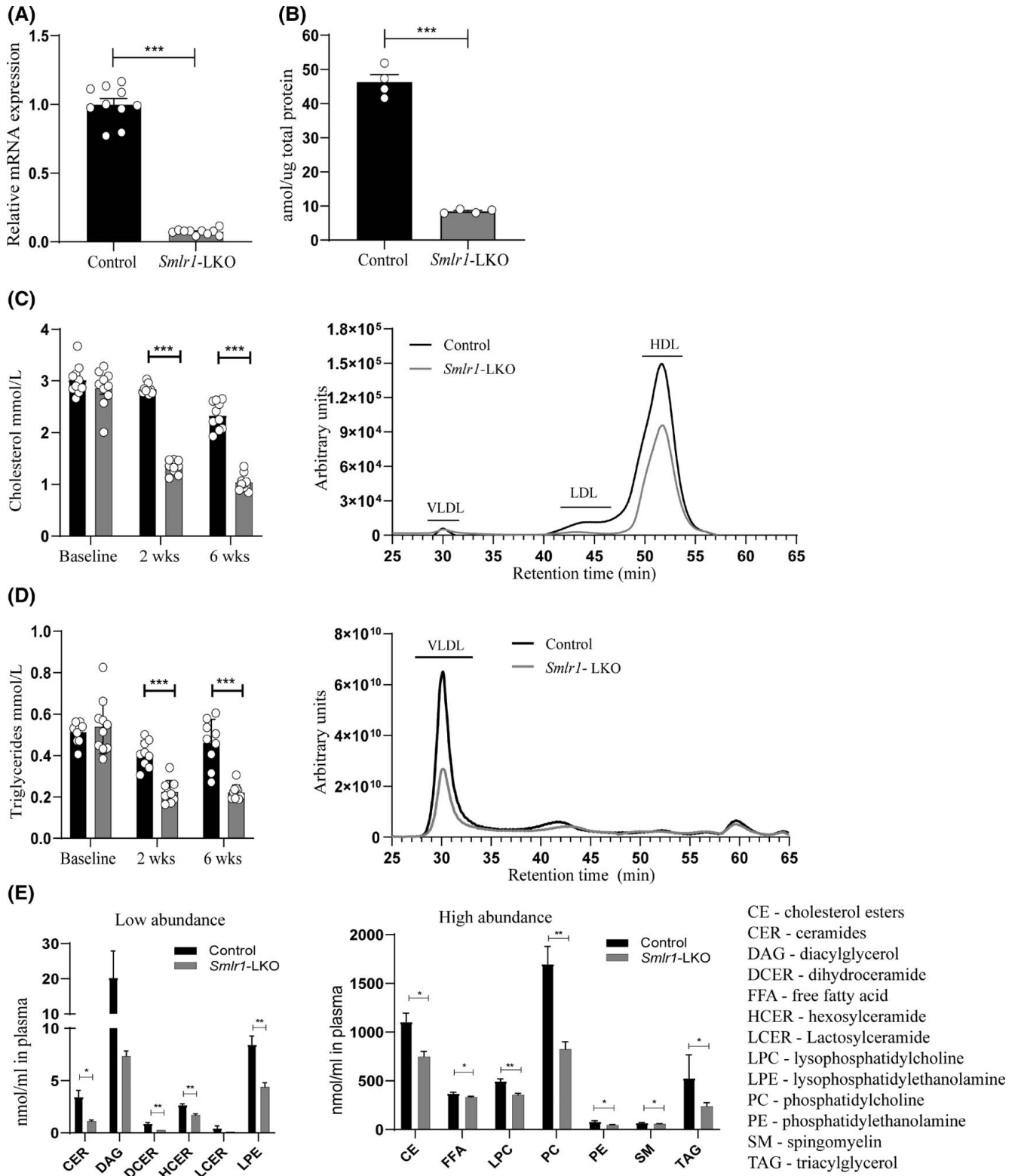


FIGURE 2 Hepatic CRISPR/Cas9-mediated small leucine-rich protein 1 (*Smlr1*) gene editing results in reduced plasma lipid levels in mice fed a chow diet. (A–E) Gene, protein, and plasma lipid levels of male Alb-Cas9 mice ($n = 20$) that received either control adeno-associated virus 8 (AAV8) or AAV8 with single-guide RNAs (sgRNAs) targeting *Smlr1* and were terminated after 6 weeks. (C,D) Fast protein liquid chromatography (FPLC) lipoprotein profiles of pooled plasma of male Alb-Cas9 mice ($n = 10$) that received either control adenovirus (AV) or AV with sgRNAs directed against *Smlr1* and were terminated after 3 weeks. Following virus application, mice were individually housed and kept on a chow diet. Data represent mean \pm SEM. (A) Hepatic *Smlr1* mRNA expression. (B) Hepatic SMLR1 protein levels of randomly selected mice ($n = 4$ per group). (C) Plasma cholesterol levels and lipoprotein cholesterol profile of pooled plasma. (D) Plasma triglyceride levels and lipoprotein triglyceride profile of pooled plasma. (E) Plasma lipidomics survey; major lipid classes are shown separately for high and low abundance. Abbreviation: *Smlr1*-LKO, *Smlr1* liver-specific knockout

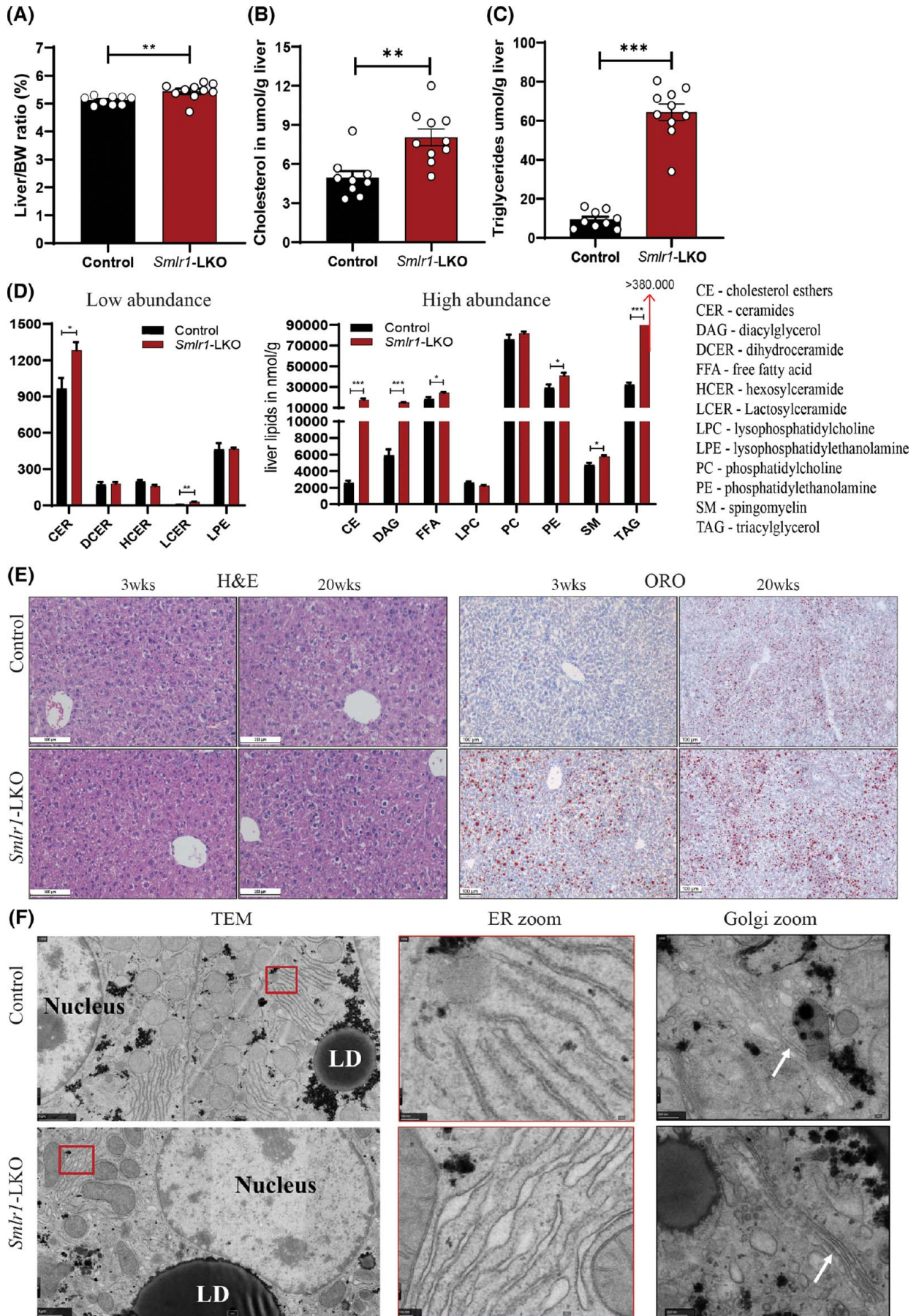


FIGURE 3 Loss of hepatic SMLR1 induces hepatic steatosis in mice on a chow diet. Liver weight, liver lipids, and histology following hepatic CRISPR/Cas9-mediated *Smlr1* gene editing. Male (Alb-Cas9) mice ($n = 5-10$) received either control AAV8 or AAV8 with sgRNAs directed against *Smlr1*. Following virus administration, mice were individually housed and kept on a chow diet. (A–D,F) Mice were terminated after 6 weeks. (E) Mice were terminated after 3 or 20 weeks. Data represent mean \pm SEM. (A) Liver to body weight (BW) ratio. (B) Hepatic cholesterol content. (C) Hepatic triglyceride content. (D) Liver lipidomics. (E) Two representative images per group of hepatic (cryo)sections stained with hematoxylin and eosin (H&E) and Oil Red O (ORO). Scale bar = 100 μ m. (F) Transmission electron microscopy (TEM) pictures showing the endoplasmic reticulum (ER) and Golgi. Scale bar from left to right is 1 μ m, 100 nm, and 200 nm. Abbreviation: LD; lipid droplet

Although phospholipid composition and abundance has been linked to NAFLD by regulating lipoprotein secretion and lipid droplets size,^[29,30] the most abundant phospholipid, phosphatidylcholine, was not altered between the study groups (Figure 3D). The rapid hepatic lipid accumulation after 3 weeks on chow diet led us to follow *Smlr1*-LKO mice for a longer period. *Smlr1*-LKO mice fed a chow diet for 20 weeks did, however, not show aggravated hepatic lipid accumulation (Figure S4D–F) without pronounced histological differences between the 3-week and 20-week groups as assessed by hematoxylin and eosin (H&E) staining of liver sections (Figure 3E). Similarly, Oil Red O staining shows similar amounts of hepatic neutral lipids in *Smlr1*-LKO mice that were sacrificed at 3 weeks and 20 weeks following viral injection (Figure 3E), suggesting that further lipid accumulation is somehow blunted during aging.

To study effects at the cellular level, we used transmission electron microscopy (TEM). In a representative section presented in Figure 3F, we noted larger lipid droplets in hepatocytes and dilated ER cisterns in *Smlr1*-LKO hepatocytes compared with controls. Other organelles like the Golgi appeared similar between the groups. In short, we note that SMLR1 plays a major role in liver lipid homeostasis, and its hepatic knockdown in mice causes steatosis within 6 weeks without notable deterioration of this phenotype at 20 weeks.

SMLR1 localizes to the ER and Golgi in immortalized human hepatocytes

To elucidate the mechanism by which hepatic SMLR1 regulates lipid levels, we performed immunofluorescence studies to identify the subcellular location of hSMLR1. To this purpose, we used immortalized human hepatocytes (IHHs). Because we identified SMLR1 through MTP, which localizes to the ER, we hypothesized that SMLR1 might also play a role in this cellular compartment. With commercially available antibodies as well as custom-made antibodies, we were not able to detect endogenous SMLR1 in hepatocarcinoma cell lines (IHH and HepG2). To examine whether hSMLR1 is in the ER, we transiently overexpressed and stained hSMLR1 and showed proximity to a calnexin antibody that appears to recognize calnexin epitopes in the lumen of the ER (Figure 4A; Figure S6). In a next step, we transiently expressed hSMLR1 fused with a FLAG tag and observed a clear overlap with an antibody that stains calnexin in the

ER membrane (Figure 4B; Figure S6). The results combined suggest that hSMLR1 is an ER-transmembrane protein. Because lipoprotein assembly and trafficking in the cell also involve the Golgi apparatus, we used GM130 (golgin A2) and p230 (golgin A4) as cis and trans-Golgi markers, respectively. Figure 4C,D shows that hSMLR1 partly colocalizes with the cis-Golgi and it aligns with the trans-Golgi markers. In further subcellular studies, we were not able to detect endogenous MTP, but we did find that hSMLR1 partially colocalized with apoB in HepG2 cells (Figure 4E). Based on these experiments, we conclude that hSMLR1 is present in the ER membrane and in the cis-Golgi, which suggests a role for SMLR1 in apoB/VLDL trafficking between the ER and the Golgi apparatus.

Hepatic SMLR1 deficiency reduces VLDL secretion

When considering the increase in liver lipids and reduction in plasma lipids in *Smlr1*-LKO mice, we hypothesized that hepatic loss of *Smlr1* may attenuate VLDL secretion. To study this, we injected Poloxamer, which blocks intravascular lipoprotein lipase-mediated hydrolysis of VLDL triglycerides. In fasted animals, this intervention resulted in markedly lower plasma triglycerides in *Smlr1*-LKO compared with control mice (Figure 5A) and a 45% reduction of the hepatic TG secretion rate (Figure 5B). In this experiment, plasma TG are used as a proxy for VLDL secretion, but these findings could also be the result of reduced intracellular lipidation of apoB. To address this possibility, we examined apoB concentration in the circulation. With an average apoB reduction of 40% (Figure 5C) and a 52% reduction in TGs in plasma of *Smlr1*-LKO mice, the TG/apoB ratios were not significantly altered, supporting the idea that SMLR1 does not affect the lipidation of apoB. Because the effects seen so far can originate from altered MTP activity or levels, we measured TAG transfer activity of MTP in liver homogenates of *Smlr1*-LKO and controls. However, no differences in MTP activity nor in protein levels were seen (Figure 5D,E; Figure S7A,B), which makes it highly unlikely that the phenotype of *Smlr1*-LKO mice was due to reduced MTP function.

VLDL also carries various exchangeable apolipoproteins, such as apoC1, apoC2, apoC3, and apoE,^[31] which were all decreased >62% in plasma of *Smlr1*-LKO mice (Table 1).

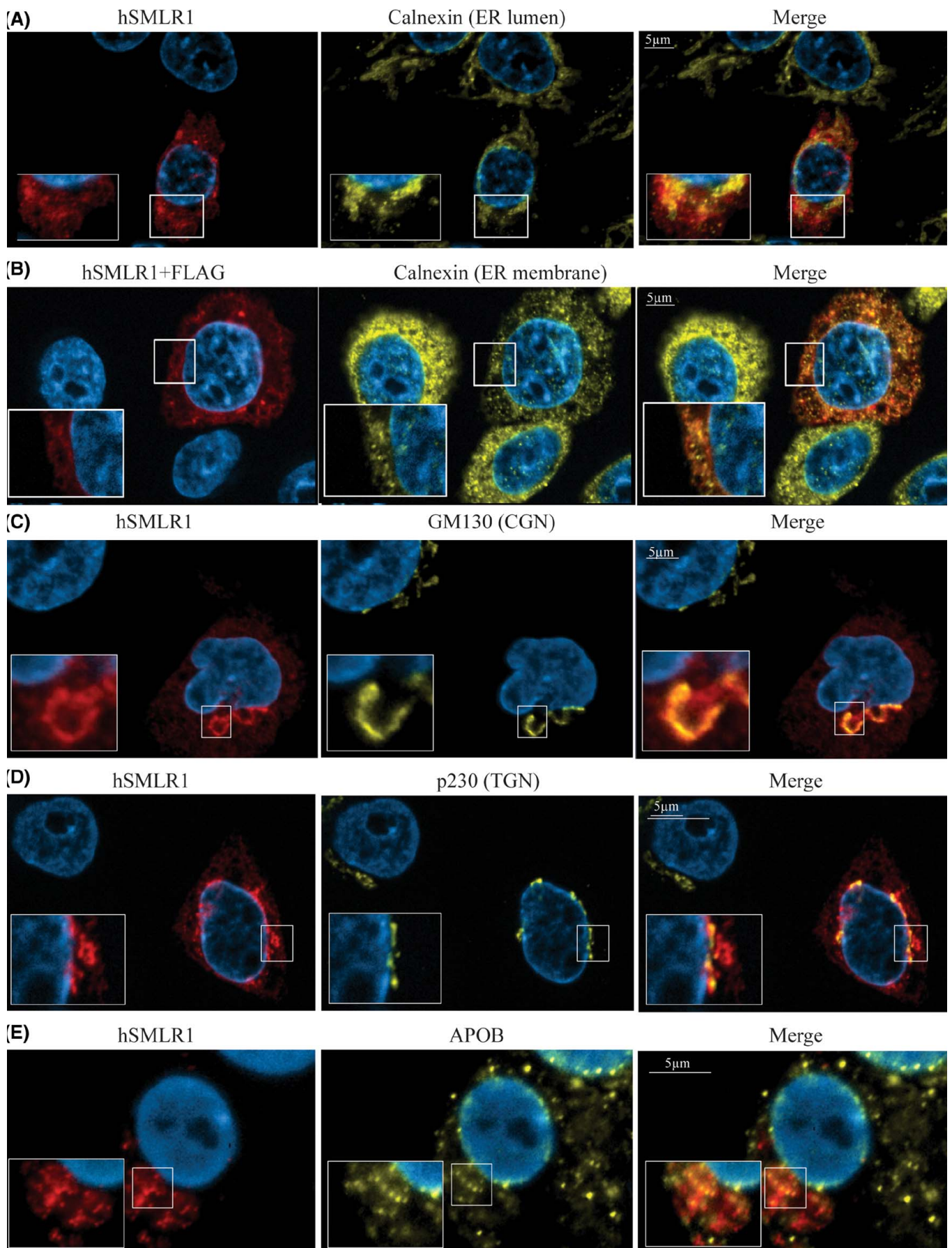


FIGURE 4 Immunofluorescence staining indicates that hSMLR1 is present in the ER membrane and cis-Golgi, where it co-localizes with apoB. Confocal fluorescence images of double-immunolabeled immortalized human hepatocytes (IHHs) or HepG2 cells in which hSMLR1 was overexpressed. Scale bar = 5 μ m. (A) Colocalization of hSMLR1 with calnexin as ER luminal marker in IHH in cells. (B) Colocalization of hSMLR1-FLAG with calnexin as ER membrane marker in IHH cells. (C) Colocalization of hSMLR1 and GM130 as cis-Golgi marker in IHH cells. (D) Colocalization of hSMLR1 and p230 as trans-Golgi marker in IHH cells. (E) Colocalization of hSMLR1 with apoB in HepG2 cells

In addition to the effects on VLDL, the *Smlr1*-LKO mice also show a drop in plasma HDL cholesterol compared with controls (Figure 2C), which is reflected by a 56% reduction of apoA1, the major apolipoprotein of HDL (Table 1). Taken together, we show that loss of hepatocyte SMLR1 reduces VLDL secretion without affecting MTP activity.

Hepatic SMLR1 deficiency protects against atherosclerosis

Because *Smlr1*-LKO mice exhibit markedly reduced cholesterol and TG levels, two independent risk factors for atherosclerosis,^[32,33] we expected that these mice would be protected against atherosclerosis. To study this, we blunted hepatic LDLR protein levels by injecting AAV8-PCSK9 encoding a gain-of-function PCSK9

variant to increase plasma lipids and sensitize mice to diet-induced atherosclerosis (Figure S8A) in *Smlr1*-LKO mice (Figure 6A) and controls. We used female mice, as these are more prone to develop atherosclerosis compared with males.^[2] The mice were fed a HFD (60%/+0.25%) for 12 weeks before sacrifice. Our studies were not designed to evaluate metabolic effects, but we noticed that, despite similar food intake, *Smlr1*-LKO mice had reduced fat mass (Figure S8B,C) and showed a trend toward reduced body weight gain (Figure 6B). *Smlr1*-LKO mice showed a marked resistance against diet-induced hyperlipidemia with 82% lower cholesterol and 88% lower plasma TG levels compared with controls (Figure 6C,D). Based on the H&E staining, *Smlr1*-LKO mice virtually did not develop atherosclerotic lesions compared with controls (Figure 6E,F). This

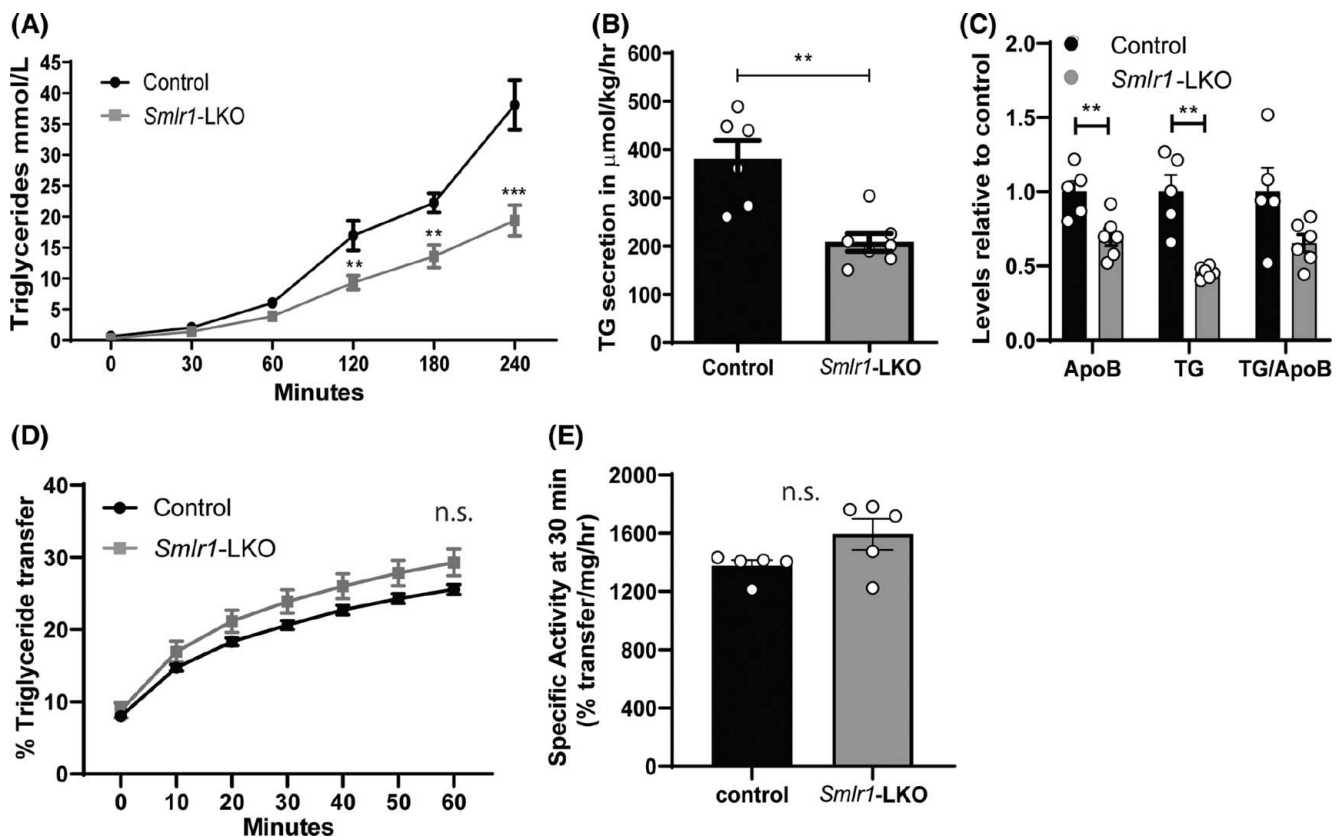


FIGURE 5 Loss of hepatic SMLR1 decreases VLDL secretion and results in lower levels of apolipoproteins. Plasma triglyceride (TG) or apolipoprotein levels following hepatic CRISPR/Cas9-mediated gene *Smlr1* gene editing. Following virus administration, mice were individually housed, kept on a chow diet, and were terminated after 6 weeks. (A,B) Female Alb-Cas9 mice ($n = 13$) received either control AV or AV with sgRNAs directed against *Smlr1*. (C-E) Male Alb-Cas9 mice ($n = 10$) that received either control AAV or AAV with sgRNAs directed targeting against *Smlr1*. Data represent mean \pm SEM. (A) Plasma TG levels in mice following poloxamer injections at 5 weeks following virus administration. (B) TG secretion rate in μ mol/kg/h, calculated from (A). (C) Relative apoB, TG, and TG/apoB ratios. (D) TG transfer activity of microsomal triglyceride transfer protein (MTP) in the liver over time. (E) TG transfer activity of MTP in the liver at 30 min. Abbreviation: n.s., not significant.

TABLE 1 Reduced levels of apolipoprotein in plasma after hepatic ablation of *Smlr1* in mice on chow

	Control mg/ dl plasma	SD	<i>Smlr1</i> -LKO mg/dl plasma	SD	<i>p</i> -value
ApoA1	308.1	67.6	135.3	42.7	0.0011***
ApoA2	46.2	9.3	14.3	8.0	0.0002***
ApoA4	39.2	10.6	32.9	6.1	0.2827n.s.
ApoC1	4.6	1.5	1.1	0.7	0.0021***
ApoC2	10.7	3.3	3.1	1.6	0.0024***
ApoC3	20.0	6.2	4.3	2.1	0.0016***
ApoC4	2.0	0.8	0.3	0.1	0.0037***
ApoD	7.6	2.6	4.2	0.64	0.0310*
ApoE	14.7	4.04	5.6	1.09	0.0032***
ApoM	5.8	1.6	2.8	0.6	0.0061**

Note: Plasma protein levels are presented as mean \pm SD. ApoC1 is presented as percentage relative value compared to controls. The mean value of $n = 5$ is presented in bold. Asterisks denote corresponding statistical significance * $p < 0.05$, ** $p < 0.005$, *** $p < 0.0005$.

experiment shows that hepatic loss of SMLR1 protects against atherosclerosis.

Hepatic SMLR1 deficiency induces NASH on an HFD

The *Smlr1*-LKO mice fed a HFD for 12 weeks had increased liver weight, liver-to-body weight ratio, and paler colored livers compared with controls (Figure 7A, Figure S8D). This matches with the 1.8-fold and 2.1-fold increases in hepatic cholesterol and TG levels, respectively, compared with controls (Figure 7D,E). Furthermore, we identified a 2-fold increase in plasma alanine aminotransferase and aspartate aminotransferase in the *Smlr1*-LKO mice compared with controls (Figure S9A). To investigate the (patho)physiological consequences in more detail, we performed histological analyses that revealed lipid accumulation in zone 3 (centrilobular) and partly in zone 2 (midzonal), which was primarily microvesicular (Figure 7D, Table S3) in *Smlr1*-LKO livers versus controls. H&E staining was further evaluated and scored using an adapted version of the NAFLD activity score (NAS), which comprises the unweighted sum of steatosis, lobular inflammation, and ballooning (Table S3). This scoring revealed a $NAS \geq 5$ for *Smlr1*-LKO mice, which correlates with the diagnosis of NASH compared with a $NAS < 3$ in the control mice, which is considered "not NASH" (Figure 7E). Sirius red staining did not show collagen deposition in both groups (Figure 7F). Despite a higher NAS, including 2.2 times more inflammatory foci per field (lobular inflammation) in hepatic SMLR1-deficient mice compared to controls, the hepatic mRNA levels of several inflammatory markers were not different from controls (Figure S9B).

To better address liver inflammation, we performed immunohistological stainings for several immune cells: CD11B (monocyte-derived macrophages), F4/80 (macrophages), B220 (B cells), and CD3 (T cells). Figure S9C,D shows a significant increase in macrophages, B cells, and T cells in livers from *Smlr1*-LKO mice compared with controls. These results therefore support the NASH score assessment. Combined, these findings suggest that *Smlr1*-LKO mice fed a HFD diet for 12 weeks can be categorized with NASH.

With no published information on the role of SMLR1 in human lipid metabolism, we analyzed an existing data set^[34] of 36 patients with different degrees of NASH and 16 controls and found that hepatic SMLR1 expression is negatively correlated with NASH grade (correlation coefficient $r = -0.42$). A second public data set of 143 patients with NASH with various degrees of fibrosis (GSE162694) supported a negative association between SMLR1 expression and NASH severity (Figure S10).

Hepatic ablation of SMLR1 does not cause disturbances in glucose homeostasis

To address whether loss of hepatic SMLR1 causes metabolic disturbances, we studied male mice, as they are more prone to develop diet-induced diabetes and insulin resistance compared with females.^[35] Information on body weight, food intake, and liver weight can be found in Figure S11A–D. Figure 8A,B shows that *Smlr1*-LKO male mice on HFD for 7–9 weeks neither develop insulin resistance nor glucose intolerance but show trends toward increased glucose sensitivity and insulin tolerance. The data combined show that NAFLD and NASH in this mouse model occur without apparent disturbances of glucose homeostasis.

DISCUSSION

We identified SMLR1 as a candidate lipid gene through contextual co-expression analyses with *MTTP* in human and murine transcriptome datasets. The SMLR1 gene has not been identified by genetic studies,^[36] which may be related to its small size. Here, we show that loss of hepatic SMLR1 in mice compromised VLDL secretion, which results in hepatic steatosis on a chow diet and NASH on HFD without disturbances of glucose homeostasis. The strong reduction in plasma lipid levels following hepatic SMLR1 ablation protects mice against atherosclerosis. Finally, subcellular studies show that SMLR1 is localized to the ER membrane and cis-Golgi network.

Our initial study showed that whole-body loss of SMLR1 is not compatible with life, which bears similarity to embryonic lethality of *Mttp* and *ApoB*-deficient

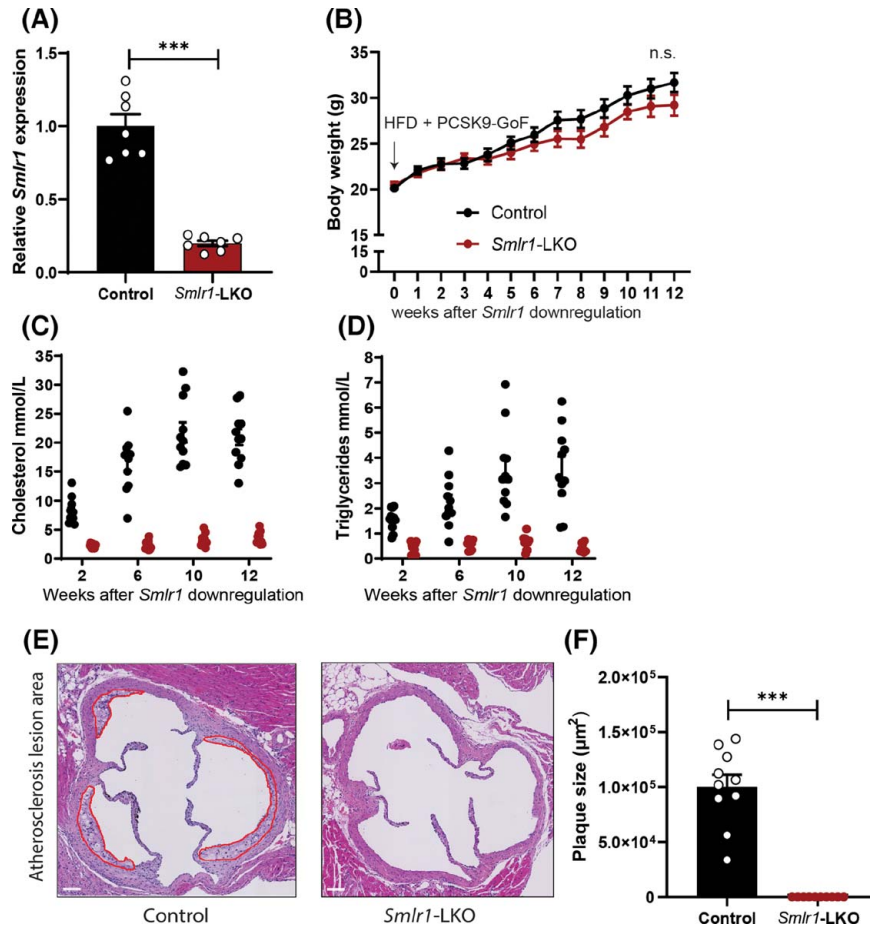


FIGURE 6 Loss of hepatic *Smlr1* protects against diet-induced atherosclerosis. Female (Alb-Cas9) mice ($n = 14\text{--}20$) received AAV with a gain-of-function (GoF) variant of PCSK9 together with either control AAV or AAV with sgRNAs directed targeting against *Smlr1*. Following virus delivery, mice were individually housed, kept on high-fat, high-cholesterol diet (HFD), and were terminated after 12 weeks. Data represent mean \pm SEM. (A) Hepatic *Smlr1* mRNA expression. (B) Weekly measured body weight. (C) Plasma total cholesterol. (D) Plasma TG levels. (E) Atherosclerotic plaque formation in the three-valve area of the heart. Representative images are shown. Scale bar = 100 μm . (F) Lesion area is the average of four cross-sections per animal. Group averages are shown.

mice.^[37,38] This is also the case for whole-body ablation of *Sar1B* and *Surf4*, which play roles in VLDL trafficking^[39,40] and suggest the importance of VLDL production during embryonic development in mice. Next, we deleted *Smlr1* in hepatocytes of adult mice, resulting in an 85% reduction of SMLR1 protein levels. When characterizing *Smlr1*-LKO mice, we noted a strong similarity with liver-specific *Mttp*^{-/-} mice^[38] with near phenocopies of the lipoprotein profiles.^[38] Loss of hepatic SMLR1 or MTP^[37] in mice results in 56% and 48% reductions in plasma cholesterol, and 52% and 72% reductions in plasma triglycerides, respectively.^[39] On the other hand, *Smlr1*-LKO mice show a 40% decrease in plasma apoB levels, whereas this is over 95% in *Mttp*-LKO mice.^[38] We considered that loss of SMLR1 could have a direct effect on MTP activity in hepatocytes, but our studies show that loss of SMLR1 does not affect MTP activity, and even increases MTP activity when the mice are fed a HFD (Figure S12A–C), supporting the idea that SMLR1 does not control MTP activity.

When the secretion of VLDL triglycerides is attenuated, one can expect TGs to accumulate in the liver.^[1] Indeed, in *Smlr1*-LKO mice fed a chow diet, hepatic TGs are approximately 7-fold increased. Based on histological examination, *Mttp*-LKO mice were initially reported to have mild hepatosteatosis,^[38] but follow-up studies show that TGs in livers are similarly 3-fold to 7-fold increased.^[27,41] As previously described for *Mttp*-LKO,^[27] *Smlr1*-LKO likewise do not show changes in glucose tolerance or insulin sensitivity. In the case of liver-specific loss of TorsinA, another factor involved in VLDL biogenesis, there are also no changes in glucose homeostasis despite hepatic steatosis on a chow diet.^[10] These examples show that hepatic steatosis due to attenuated VLDL secretion can occur in the context of normal glucose homeostasis. There are, however, differences when it comes to hepatic pathology: Liver-specific loss of TorsinA results in severe NASH (NAS score of 6) when mice are fed a chow diet for 6 months, whereas *Smlr1*-LKO mice develop NASH when fed a HFD diet

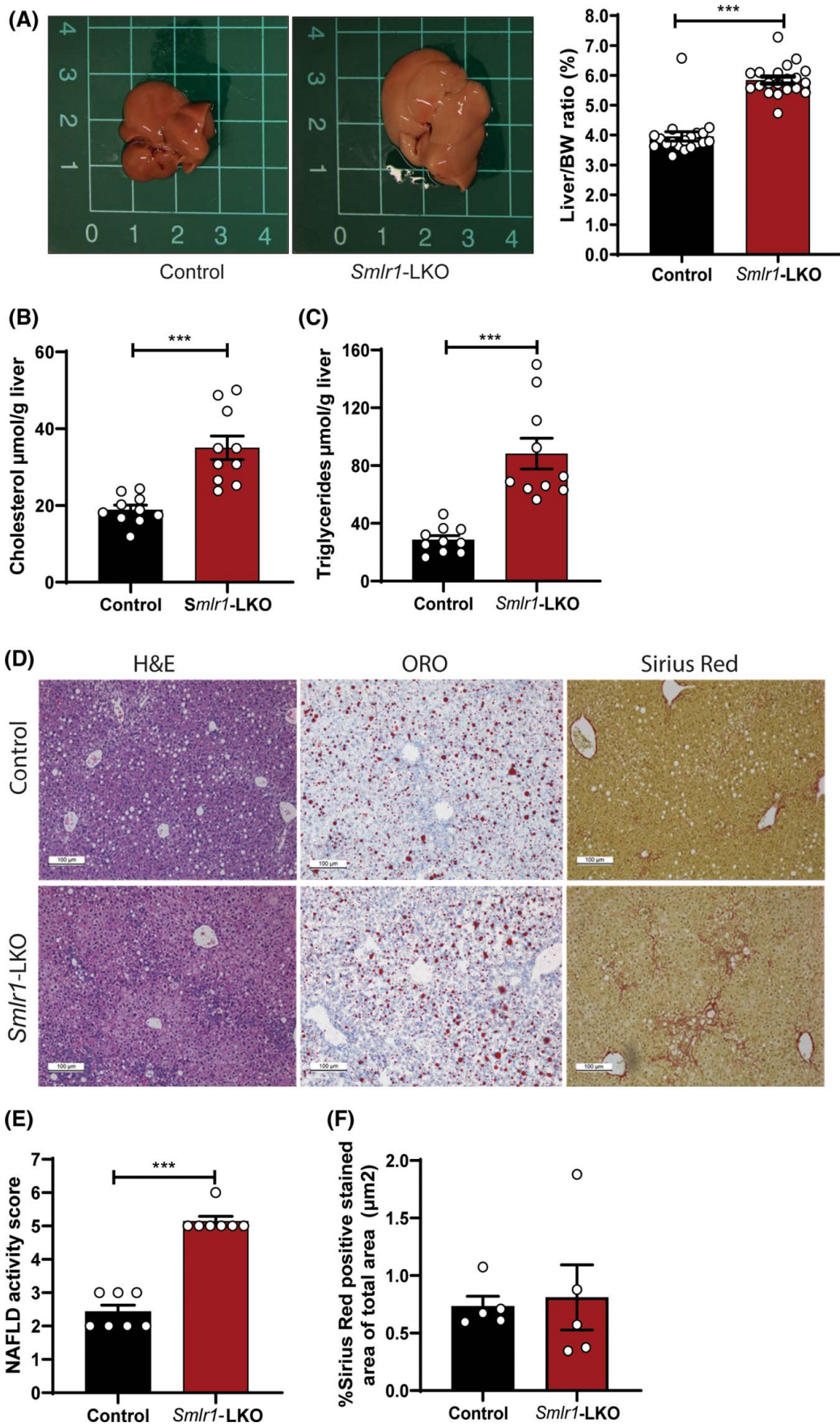


FIGURE 7 Loss of hepatic *Smlr1* is associated with increased NAFLD on HFD. Female (Alb-Cas9) mice ($n = 14$) received AAV with a gain-of-function variant of PCSK9 together with either control AAV or AAV with sgRNAs directed targeting against *Smlr1*. Following virus administration, mice were individually housed, kept on HFD, and were terminated after 12 weeks. Data represent mean \pm SEM ($n = 14$ –39). (A) Left: Two representative images of the liver following sacrifice (ruler is in centimeters). Right: Liver to BW ratio. (B) Hepatic cholesterol content. (C) Hepatic TG content. (D) Representative images of immunohistological staining (H&E, ORO, sirius red). Scale bar = 100 μ m. (E) NAFLD activity score. (F) Sirius red staining expressed as percentage positive area of total area (μ m² field).

for 3 months (NAS score ≥ 5). The hepatic loss of SAR1B or SURF4 both play a role in the trafficking of VLDL from the ER to the Golgi, only cause a 3-fold increase in hepatic TGs in mice on a chow diet, but with an intriguing near absence of TGs and apoB in plasma.^[16] The absence of an association between the degree of steatosis and plasma TGs can be attributed to changes in beta-oxidation, ER stress, and autophagy in some of these mouse models.^[10,42] Taken together, studies in mice show that hepatic loss of apoB, MTP, SURF4, SAR1B, torsinA, and SMLR1 all result in hepatic steatosis and reduced TG secretion, but direct comparisons are difficult due to differences in experimental conditions, such as the length of exposure to different diets.

In a next step, we performed subcellular localization studies, which showed that SMLR1 is in the ER membrane as well as the cis-Golgi network. SAR1B also localizes to the ER and the Golgi, where it plays a role in Coatamer protein complex II transport for proteins as well as VTVs.^[15] More specifically, SAR1B acts together with SURF4 to mediate the transport of VLDL out of the ER to the Golgi network.^[16] Furthermore, hepatic loss of SURF4 causes dilated ER and accumulation of lipoproteins in the ER. Although we also noted dilated ER in SMLR1-deficient hepatocytes, we did not observe an accumulation of lipoproteins in the ER. Another player in VLDL assembly is TMEM41B, an ER lipid scramblase that translocates phospholipids between monolayers of the ER^[8] for maturing lipoproteins as well as equilibrating ER leaflets following ER budding of VTVs. Mice lacking hepatic TMEM41B present attenuated VTV

transport and >50% lower VLDL secretion but also without apparent accumulation of lipoproteins in the ER.^[8] The recent identification of players in the VLDL secretion pathway, now including SMLR1, illustrates the tight regulation of VLDL trafficking throughout the cell and their strong impact on hepatic lipid homeostasis.

While numerous proteins affect the trafficking of VLDL, other proteins control the delivery of TGs from intracellular lipid droplets to apoB for lipidation. For example, *Tm6sf2*^{-/-} in mice results in a 2-fold increase in hepatic TGs and reduced TG-rich VLDL in the circulation without changes in apoB levels on a chow diet.^[43] While TM6SF2 is not known to play a role in apoB trafficking, it is, like SMLR1, present in the ER and Golgi.^[43] One could, in this regard, hypothesize a role for SMLR1 in stabilizing TM6SF2, like what is described for small ER lipid raft proteins 1 and 2.^[11] However, whether apoB levels are affected in *Tm6sf2*^{-/-} mice is debated,^[11,43] whereas loss of hepatic SMLR1 ablation strongly reduces plasma apoB levels. Taken together, we postulate a role for SMLR1 in VLDL trafficking.

Our study has limitations. First, we have attributed the plasma lipid phenotype of our *Smlr1*-LKO mice to decreased VLDL output but have not ruled out the possibility of increased hepatic uptake. However, the remarkable resistance of these mice to diet-induced dyslipidemia despite PCSK9-mediated ablation of the LDLR makes this unlikely. Second, we still have little knowledge of the role of SMLR1 in human liver lipid metabolism. Genetic epidemiological analyses are in this regard problematic due to apparent lack of

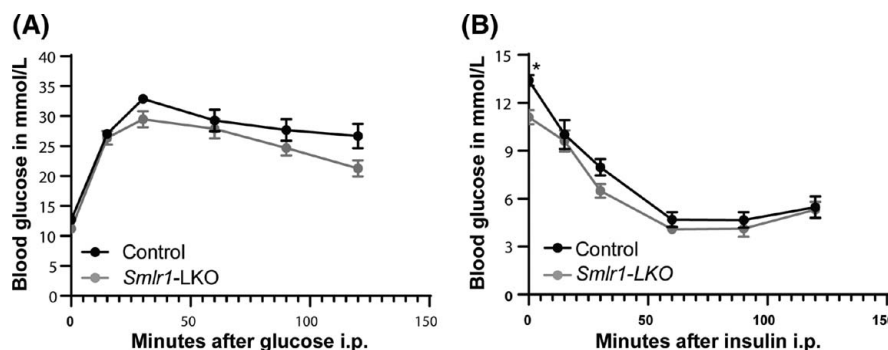


FIGURE 8 Loss of hepatic *Smlr1* does not alter glucose homeostasis on HFD. Male (Alb-Cas9) mice ($n = 19$) received control AAV or AAV with sgRNAs directed targeting against *Smlr1*. Following virus administration, mice were individually housed, kept on HFD, and were terminated after 13 weeks. Data represent mean \pm SEM. (A) Blood glucose levels following intraperitoneal injection of glucose after 7 weeks on HFD. (B) Blood glucose levels following intraperitoneal injection of insulin after 9 weeks on HFD

affected SMLR1 function or expression by polymorphisms in the *SMLR1* gene locus. Finally, the exact mechanism by which SMLR1 may facilitate cargo transport of apoB in hepatocytes warrants further in-depth studies.

Studies in the public domain show that *Smlr1* has not been identified either by genome-wide association study nor co-immunoprecipitation studies. Here we show that sophisticated analysis of transcriptomic data sets is yet another tool to identify previously unknown players in lipid homeostasis. Our study presents SMLR1 as a player in VLDL trafficking. Loss of hepatic SMLR1 increases hepatic lipids, decreases plasma lipids, and protects against atherosclerosis without disturbing glucose homeostasis. It closely matches studies of the hepatic loss of other factors of the VLDL production machinery, like apoB and MTP. This phenotype contrasts with an obesity-driven increased VLDL production, insulin resistance, hepatic lipid accumulation, as well as increased risk of atherosclerosis that is commonly studied in the field of hepatology. We believe that fundamental research into VLDL biogenesis will aid in the development of drugs to treat liver steatosis as well as atherosclerosis in patients who suffer from the consequences of obesity.

AUTHOR CONTRIBUTIONS

Experiments: Willemien van Zwol and Antoine Rimbart. *Targeted proteomics:* Justina C. Wolters. *Experimental support:* Marieke Smit, Niels J. Kloosterhuis, Nicolette C. A. Huijman, and Umesh Tharehalli. *Human data sets and preliminary work:* Vincent W. Bloks. *Histology staining:* Mirjam H. Koster. *Histopathological analyses:* Simon M de Neck and Alain de Bruin. *Lipodomics:* Joerg Heeren, Marceline M. Fuh, and Ludger Scheja. *Transmission electron microscopy:* Jeroen Kuipers. *MTTP assays:* Sujith Rajan. *3D model design:* Colin Bournez. *Materials and resources for 3D modeling:* Gerard J. P. van Westen. *Study design, analysis, and data interpretation:* Willemien van Zwol, Jan Albert Kuivenhoven, and Bart van de Sluis. *Manuscript draft:* Willemien van Zwol, Antoine Rimbart, Philip Zimmerman, Bart van de Sluis, and Jan Albert Kuivenhoven. *Critical review of the manuscript:* Henry N. Ginsberg, M. Mahmood Hussain. *Research supervision:* Jan Albert Kuivenhoven. All authors reviewed and revised the manuscript.

ACKNOWLEDGMENT

The authors thank M. Heidenfelder for the manuscript editing, L. Larsen for the technical support, and JF de Boer for his valuable input and assistance with data analyses.

CONFLICTS OF INTEREST

Nothing to report.

DATA AVAILABILITY STATEMENT

Dataset used: GSE162694 (is cited in the text) available on: <https://www.ncbi.nlm.nih.gov/geo/query/acc.cgi?acc=GSE162694>

ORCID

Willemien van Zwol  <https://orcid.org/0000-0003-2298-6563>

Antoine Rimbart  <https://orcid.org/0000-0002-2971-4926>

Gerard J. P. van Westen  <https://orcid.org/0000-0003-0717-1817>

REFERENCES

- Di Filippo M, Moulin P, Roy P, Samson-Bouma ME, Collardeau-Frachon S, Chebel-Dumont S, et al. Homozygous MTTP and APOB mutations may lead to hepatic steatosis and fibrosis despite metabolic differences in congenital hypocholesterolemia. *J Hepatol.* 2014;61:891–902.
- Peloso GM, Nomura A, Khera AV, Chaffin M, Won HH, Ardissino D, et al. Rare protein-truncating variants in APOB, lower low-density lipoprotein cholesterol, and protection against coronary heart disease. *Circ Genom Precis Med.* 2019;12:e002376.
- Higuchi N, Kato M, Tanaka M, Miyazaki M, Takao S, Kohjima M, et al. Effects of insulin resistance and hepatic lipid accumulation on hepatic mRNA expression levels of apoB, MTP and L-FABP in non-alcoholic fatty liver disease. *Exp Ther Med.* 2011;2:1077–81.
- Zhang Z, Zong C, Jiang M, Hu H, Cheng X, Ni J, et al. Hepatic HuR modulates lipid homeostasis in response to high-fat diet. *Nat Commun.* 2020;11:3067.
- Pullinger CR, North JD, Teng BB, Rifci VA, Ronhild de Brito AE, Scott J. The apolipoprotein B gene is constitutively expressed in HepG2 cells: regulation of secretion by oleic acid, albumin, and insulin, and measurement of the mRNA half-life. *J Lipid Res.* 1989;30:1065–77.
- Wu JX, He KY, Zhang ZZ, Qu YL, Su XB, Shi Y, et al. L2P is required for hepatic triacylglycerol transportation through maintaining apolipoprotein B stability. Qi L, editor. *PLOS Genetics.* 2021;17:e1009357.
- Sirwi A, Hussain MM. Lipid transfer proteins in the assembly of apoB-containing lipoproteins. *J Lipid Res.* 2018;59:1094–2.
- Huang D, Xu B, Liu L, Wu L, Zhu Y, Ghanbarpour A, et al. TMEM41B acts as an ER scramblase required for lipoprotein biogenesis and lipid homeostasis. *Cell Metab.* 2021;33:1655–70.e8.
- Peng H, Chiu TY, Liang YJ, Lee CJ, Liu CS, Suen CS, et al. PRAP1 is a novel lipid-binding protein that promotes lipid absorption by facilitating MTTP-mediated lipid transport. *J Biol Chem.* 2021;296:100052.
- Shin JY, Hernandez-Ono A, Fedotova T, Östlund C, Lee MJ, Gibeley SB, et al. Nuclear envelope-localized torsinA-LAP1 complex regulates hepatic VLDL secretion and steatosis. *J Clin Invest.* 2019;129:4885–900.
- Li BT, Sun M, Li YF, Wang JQ, Zhou ZM, Song BL, et al. Disruption of the ERLIN-TM6SF2-APOB complex destabilizes APOB and contributes to non-alcoholic fatty liver disease. *PLoS Genetics.* 2020;16:1–20.
- Heeren J, Scheja L. Metabolic-associated fatty liver disease and lipoprotein metabolism. *Mol Metab.* 2021;50:101238.
- Jiang X, Fulte S, Deng F, Chen S, Xie Y, Chao X, et al. Lack of VMP1 impairs hepatic lipoprotein secretion and promotes nonalcoholic steatohepatitis. *J Hepatol.* 2022;77:619–31.

14. Borén J, Adiels M, Björnson E, Matikainen N, Söderlund S, Rämö J, et al. Effects of TM6SF2 E167K on hepatic lipid and very low-density lipoprotein metabolism in humans. *JCI Insight*. 2020;175:e144079.
15. Tiwari S, Siddiqi SA. Intracellular trafficking and secretion of VLDL. *Arterioscler Thromb Vasc Biol*. 2012;32:1079–86.
16. Wang X, Wang H, Xu B, Huang D, Nie C, Pu L, et al. Receptor-mediated export of lipoproteins controls lipid homeostasis in mice and humans. *Cell Metab*. 2021;33:350–66.e7.
17. Siddiqi S, Zhelyabovska O, Siddiqi SA. Reticulon 3 regulates very low density lipoprotein secretion by controlling very low density lipoprotein transport vesicle biogenesis. *Can J Physiol Pharmacol*. 2018;96:668–75.
18. Rahim A, Nafi-valencia E, Siddiqi S, Basha R, Runyon CC, Siddiqi SA. Proteomic analysis of the very low density lipoprotein (VLDL) transport vesicles. *J Proteomics*. 2012;75:2225–35.
19. Siddiqi SA, Siddiqi S, Mahan J, Peggs K, Gorelick FS, Mansbach CM. The identification of a novel endoplasmic reticulum to Golgi SNARE complex used by the prechylomicron transport vesicle. *J Biol Chem*. 2006;281:20974–82.
20. Loaiza N, Hartgers ML, Reeskamp LF, Balder JW, Rimbart A, Bazioti V, et al. Taking one step back in familial hypercholesterolemia. *Arterioscler Thromb Vasc Biol*. 2020;40:973–85.
21. Fedoseienko A, Wijers M, Wolters JC, Dekker D, Smit M, Huijckman N, et al. The COMMD family regulates plasma LDL levels and attenuates atherosclerosis through stabilizing the CCC complex in endosomal LDLR trafficking. *Circ Res*. 2018;122:1648–60.
22. Björklund MM, Hollensen AK, Hagensen MK, Dagnæs-Hansen F, Christoffersen C, Mikkelsen JG, et al. Induction of atherosclerosis in mice and hamsters without germline genetic engineering. *Circ Res*. 2014;114:1684–9.
23. van Dam S, Vösa U, van der Graaf A, Franke L, de Magalhães JP. Gene co-expression analysis for functional classification and gene-disease predictions. *Brief Bioinformatics*. 2018;19:575–92.
24. Eisen MB, Spellman PT, Brown PO, Botstein D. Cluster analysis and display of genome-wide expression patterns. *Proc Natl Acad Sci*. 1998;95:14863–8.
25. Dominiczak MH, Caslake MJ. Apolipoproteins: metabolic role and clinical biochemistry applications. *Ann Clin Biochem*. 2011;48:498–515.
26. Guan M, Qu L, Tan W, Chen L, Wong CW. Hepatocyte nuclear factor-4 alpha regulates liver triglyceride metabolism in part through secreted phospholipase A2 GXIIB. *Hepatology*. 2011;53:458–66.
27. Minehira K, Young SG, Villanueva CJ, Yetukuri L, Oresic M, Hellerstein MK, et al. Blocking VLDL secretion causes hepatic steatosis but does not affect peripheral lipid stores or insulin sensitivity in mice. *J Lipid Res*. 2008;49:2038–44.
28. Kawano Y, Cohen DE. Mechanisms of hepatic triglyceride accumulation in non-alcoholic fatty liver disease. *J Gastroenterol*. 2013;48:434–1.
29. Li Z, Agellon LB, Allen TM, Umeda M, Jewell L, Mason A, et al. The ratio of phosphatidylcholine to phosphatidylethanolamine influences membrane integrity and steatohepatitis. *Cell Metab*. 2006;3:321–1.
30. van der Veen JN, Kennelly JP, Wan S, Vance JE, Vance DE, Jacobs RL. The critical role of phosphatidylcholine and phosphatidylethanolamine metabolism in health and disease. *Biochim Biophys Acta Biomembr*. 2017;1859:1558–72.
31. Gordon SM, Li H, Zhu X, Shah AS, Lu LJ, Davidson WS. A comparison of the mouse and human lipoproteome: suitability of the mouse model for studies of human lipoproteins. *J Proteome Res*. 2015;14:2686–95.
32. Ginsberg HN, Packard CJ, Chapman MJ, Borén J, Aguilar-Salinas CA, Averna M, et al. Triglyceride-rich lipoproteins and their remnants: metabolic insights, role in atherosclerotic cardiovascular disease, and emerging therapeutic strategies—a consensus statement from the European Atherosclerosis Society. *Euro Heart J*. 2021;42:4791–806.
33. Ference BA, Ginsberg HN, Graham I, Ray KK, Packard CJ, Bruckert E, et al. Low-density lipoproteins cause atherosclerotic cardiovascular disease. 1. Evidence from genetic, epidemiologic, and clinical studies. A consensus statement from the European Atherosclerosis Society Consensus Panel. *Euro Heart J*. 2017;38:2459–72.
34. Atanasovska B, Rensen SS, Marsman G, Shiri-Sverdlov R, Withoff S, Kuipers F, et al. Long non-coding RNAs involved in progression of non-alcoholic fatty liver disease to steatohepatitis. *Cells*. 2021;10:1–15.
35. Tramunt B, Smati S, Grandgeorge N, Lenfant F, Arnal JF, Montagner A, et al. Sex differences in metabolic regulation and diabetes susceptibility. *Diabetologia*. 2020;63:453–61.
36. Klarin D, Damrauer SM, Cho K, Sun YV, Teslovich TM, Honerlaw J, et al. Genetics of blood lipids among ~300,000 multi-ethnic participants of the Million Veteran Program. *Nat Genet*. 2018;50:1514–23.
37. Farese RV, Ruland SL, Flynn LM, Stokowski RP, Young SG. Knockout of the mouse apolipoprotein B gene results in embryonic lethality in homozygotes and protection against diet-induced hypercholesterolemia in heterozygotes. *Proc Natl Acad Sci U S A*. 1995;92:1774–8.
38. Raabe M, Véniant MM, Sullivan MA, Zlot CH, Björkegren J, Nielsen LB, et al. Analysis of the role of microsomal triglyceride transfer protein in the liver of tissue-specific knockout mice. *J Clin Invest*. 1999;103:1287–98.
39. Auclair N, Sané AT, Ahmarani L, Patey N, Beaulieu JF, Peretti N, et al. Sar1b mutant mice recapitulate gastrointestinal abnormalities associated with chylomicron retention disease. *J Lipid Res*. 2021;62:100085.
40. Emmer BT, Lascuna PJ, Tang VT, Kotnik EN, Saunders TL, Khoriaty R, et al. Murine Surf4 is essential for early embryonic development. *Herault Y, editor. PLOS ONE*. 2020;15:e0227450.
41. Newberry EP, Xie Y, Kennedy SM, Graham MJ, Croke RM, Jiang H, et al. Prevention of hepatic fibrosis with liver microsomal triglyceride transfer protein deletion in liver fatty acid binding protein null mice. *Hepatology*. 2017;65:836–52.
42. Conlon DM, Thomas T, Fedotova T, Hernandez-Ono A, Di Paolo G, Chan RB, et al. Inhibition of apolipoprotein B synthesis stimulates endoplasmic reticulum autophagy that prevents steatosis. *J Clin Invest*. 2016;126:3852–67.
43. Smagris E, Gilyard S, BasuRay S, Cohen JC, Hobbs HH. Inactivation of Tm6sf2, a gene defective in fatty liver disease, impairs lipidation but not secretion of very low density lipoproteins. *J Biol Chem*. 2016;291:10659–76.

How to cite this article: van Zwol W, Rimbart A, Wolters JC, Smit M, Bloks VW, Kloosterhuis NJ, et al. Loss of hepatic SMLR1 causes hepatosteatosis and protects against atherosclerosis due to decreased hepatic VLDL secretion. *Hepatology*. 2023;78:1418–1432. <https://doi.org/10.1002/hep.32709>